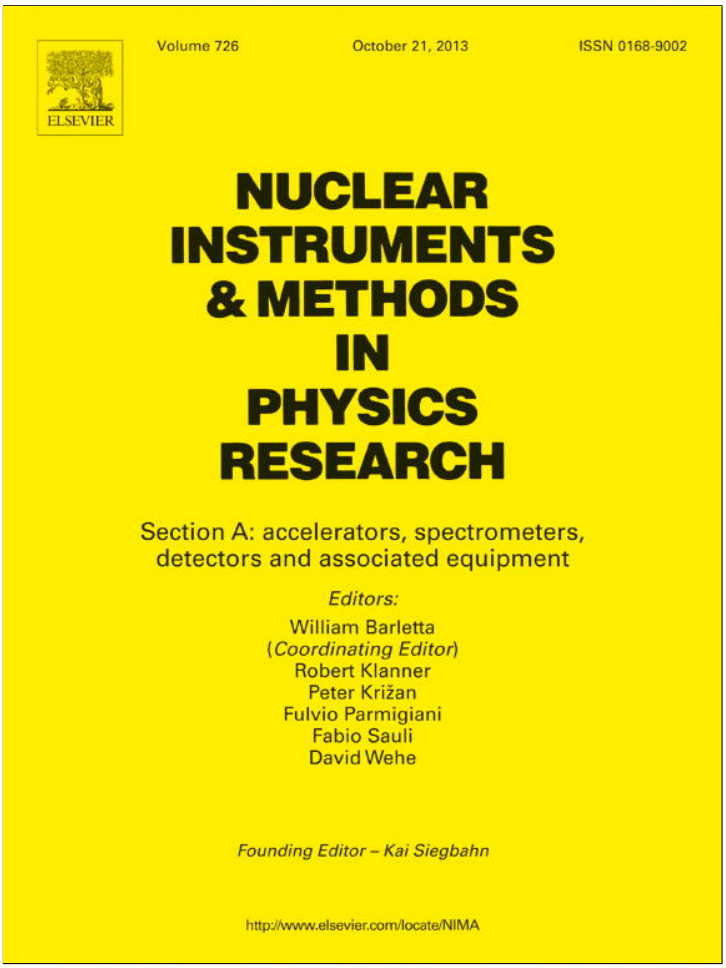

Nuclear Instruments and Methods in Physics Research A 726 (2013) 116–119

Contents lists available at SciVerse ScienceDirect

Nuclear Instruments and Methods in Physics Research A

journal homepage: www.elsevier.com/locate/nima

A detection system with broad angular acceptance for particle identification and angular distribution measurements

P.F.F. Carnelli [a,b,c,*], A. Arazi [a,b], J.O. Fernández Niello [a,b,c], O.A. Capurro [a], M.A. Cardona [a,b,c], E. de Barbará [a], J.M. Figueira [a,b], D. Hojman [a,b], G.V. Martí [a], D. Martinez Heimann [a,b], A.E. Negri [a,b], A.J. Pacheco [a,b]

[a] Laboratorio TANDAR, Comisión Nacional de Energía Atómica, Av. Gral. Paz 1499, B1650KNA, San Martín, Buenos Aires, Argentina
[b] Consejo Nacional de Investigaciones Científicas y Técnicas, Av. Rivadavia 1917, C1033AAJ, Buenos Aires, Argentina
[c] Universidad Nacional de San Martín, Campus Miguelete, B1650BWA, San Martín, Buenos Aires, Argentina

ARTICLE INFO

Article history:
Received 8 February 2013
Received in revised form
29 May 2013
Accepted 30 May 2013
Available online 6 June 2013

Keywords:
Ionization chamber
Position-sensitive detector
Angular distribution
Particle identification
Straggling
^{7}Li+^{27}Al

ABSTRACT

A new detection system for time-optimized heavy-ion angular distribution measurements has been designed and constructed. This device is composed by an ionization chamber with a segmented-grid anode and three position-sensitive silicon detectors. This particular arrangement allows identifying reaction products emitted within a 30° wide angular range with better than 1° angular resolution. As a demonstration of its capabilities, angular distributions of the elastic scattering cross-section and the production of alpha particles in the ^{7}Li+^{27}Al system, at an energy above the Coulomb barrier, are presented.

1. Introduction

Nuclear reactions produce different nuclides with a wide range of energies and scattering angles. The experimental study of the mechanisms involved in these reactions usually needs the systematic measurement of complete angular distributions of the reaction products at several energies, which implies time-consuming experiments. This situation is particularly extreme, for example, in the case of nuclear reactions induced by radioactive ion beams or those having low cross-sections, in which the optimization of all detection parameters is required, the detection efficiency being one of the most critical. In addition, the nuclear species of interest have to be identified among the background events, which are usually much more abundant. The classification of particles in terms of their atomic number Z and mass number A is usually done by measuring their partial energy-loss (ΔE) and residual energy (E_{res}) [1]. The determination of the angular distribution of the emitted particles, in turn, can be accomplished using a single movable detector, an array of several detectors, or a detector with sensitivity to the incident position.

The detection system presented in this communication was specially designed and constructed for our research program on breakup reactions induced by weakly bound nuclei. It has a large acceptance angle and the capabilities of particle identification and incidence position determination. In this device, particles go through an ionization chamber with two separated anodes (which yield ΔE_1 and ΔE_2 signals) and they are stopped at one of the three position-sensitive silicon detectors (PSD), which give the energy signal $E_{res}^{\ i}$ (i=A, B or C). In addition, each PSD provides a signal which is proportional to the particle incidence position along its active strip, x^i [1]. By time coincidence, the four non-zero signals induced by each single particle (ΔE_1, ΔE_2, $E_{res}^{\ i}$, x^i) are associated as an event. The scattering angle of each particle is then calculated from the detection system angular position and the x^i signal. In this way, the detection system allows the particle identification and the determination of its scattering angle (within a range of 30°) out of just eight electronic signals (two partial energy losses, plus the six signals provided by the PSDs). This requires the use of a limited amount of electronic modules and a single octal ADC.

Following, in Section 2, a detail of the main design and construction features of this new detection system is given. Section 3 concerns the characterization tests with several ion

* Corresponding author at: Laboratorio TANDAR, Comisión Nacional de Energía Atómica, Av. Gral. Paz 1499, B1650KNA, San Martín, Buenos Aires, Argentina. Tel.: +54 1167727101; fax: +54 1167727121.
E-mail address: carnelli@tandar.cnea.gov.ar (P.F.F. Carnelli).

0168-9002/$ - see front matter © 2013 Elsevier B.V. All rights reserved.
http://dx.doi.org/10.1016/j.nima.2013.05.182

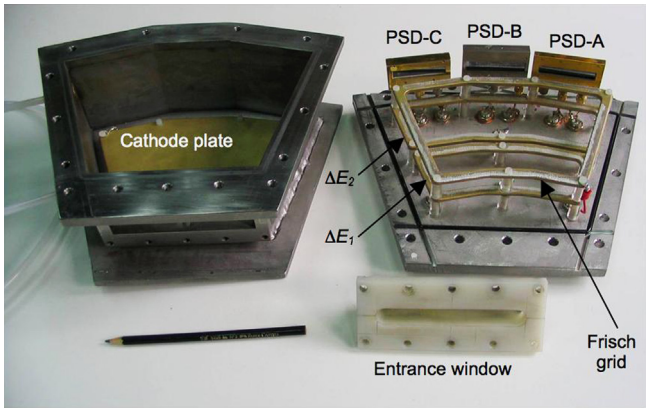

Fig. 1. Upper (on the left) and lower (on the right) pieces of the container. ΔE_1 and ΔE_2 are the two segments of the ionization chamber anode. On the back, the three PSDs are placed.

beams and the measurements performed in the ^{7}Li+^{27}Al system. Finally, conclusions and perspectives are presented in Section 4.

2. Design and construction

The detection system consists of a segmented-anode ionization chamber containing three PSDs, which are focused to the reaction-center (see Fig. 1). The device is able to discriminate different types of particles in an almost continuous 30° angular range except for two dead zones between the PSDs, of about 1° each. The advantage of having two anode segments is to provide additional discrimination of particles heavier than the ones of interest, which do not reach the PSDs. Depending on gas pressure; those particles can be either stopped at the first segment or identified by the ΔE_1–ΔE_2 correlation. On the contrary, lighter particles are better identified by the ΔE_2–E_{res} correlation. Alternatively, it is possible to shortcut the ΔE_1 and ΔE_2 output connectors to use the two anode segments as a unique ΔE detector.

The system is housed in a stainless steel case. The segmented-anode, the Frisch-grid and the PSDs are attached to the case bottom and the cathode and entrance window to the top (Fig. 1). It has an adjustable base, which allows its alignment relative to the reaction plane by means of three leveling screws. The container and its base were designed to fit in the ORTEC reaction-chamber (76 cm of internal diameter, and 25 cm of height), mounted in one of the experimental lines of the 20 UD TANDAR tandem accelerator facility. Nevertheless, the design is versatile enough to be used in other facilities.

Different commercial brand PSDs may be connected to the system. In this work, PSD A is an ORTEC P-055-0847-500 (47 mm long by 8 mm high active area, 500 μm depth), and PSDs B and C are Canberra PF1RT-50*10-300RM (50 by 10 mm^2 active area, 300 μm depth).

In order to improve the charge collection, the segmented-anode is composed of grids of 28 μm diameter gold-coated tungsten wires (2 mm separation between them). In the vicinity of the wires the electric field is strengthened, improving the output signal in contrast with usual anode plates [2]. The cathode is made of a 3 mm thick and 110 mm long bronze plate, sharing the same shape and dimensions of the Frisch-grid. The cathode, Frisch-grid and anode segments follow the container geometry (Fig. 1) and the vertical gap between each of them is 30 mm.

The entrance window of the detector is a 104 by 8 mm^2 slot made in an acryl glass frame. It is placed at 100 mm from the reaction-center and is covered by a 6.3 μm thick Mylar film. The slot determines an active solid angle of 80 msr. There is virtually no dead gap between the slot and the first anode segment (which avoids passive energy losses). Meanwhile, the dead gap between anode segments is about 5 mm and between the second segment and the PSDs is 3 mm.

3. Characterization and performance

This detection system was conceived to minimize the time required to obtain angular distributions of different reaction products. In order to characterize the device and its capabilities for this kind of measurements, it is necessary to evaluate the uncertainties that the ionization chamber gas introduce in the determination of the energy and the emission angle of the particles that are being detected. For this purpose several tests have been performed using a triple radioactive alpha source and different beams provided by the TANDAR accelerator. The performance of the detector has also been tested through the comparison of measured elastic scattering cross-sections for the ^{7}Li+^{27}Al system with previous experimental results. Moreover, an angular distribution of the alpha particles produced in this reaction system has also been obtained.

3.1. Energy and angular resolutions

The first evaluations of the energy and angular resolutions were carried out detecting alpha particles emitted by a ^{239}Pu (5.155 MeV)–^{241}Am (5.486 MeV)–^{244}Cm (5.805 MeV) alpha source and by the elastically scattered ions produced in the bombardment of a ^{197}Au target using ^{7}Li (20 MeV), ^{16}O (30 and 70 MeV), and ^{32}S (90 MeV) projectiles. In what follows, the quoted resolution corresponds to upper limits of the results obtained in the different measurements. In first place, the intrinsic relative energy resolutions of the PSDs, obtained as the FWHM/centroid ratio of the energy peaks, were found to be about 1.5% (at high vacuum). The uncertainty of the measured energy due to the straggling process in P10 gas increased at a pressure of 267 mbar, giving a FWHM/centroid ratio of 3% for the PSDs. The corresponding values for the ΔE resolutions obtained for the ionization chamber were 11.5% (5%) for the first (second) segment at 70 mbar and 8.5% (3.5%) at 270 mbar.

Several factors affect the overall uncertainty in the determination of the original emission angle of a given particle that comes from the target and is detected by the device. The most relevant are: (i) the angular straggling in the target, (ii) the angular straggling in the Mylar film of the entrance window, (iii) the angular straggling in the ionization chamber gas at a pressure P, and (iv) the position resolution of the PSDs. The corresponding uncertainties are represented by the FWHMs σ_t, σ_w, $\sigma_{gas}(P)$, and σ_{psd}, respectively, which are added in quadrature to produce a total angular uncertainty $\sigma(P)$. Among the quoted factors we will concentrate on the last three, which are inherent to the detection system.

The measurements of the intrinsic position resolutions of the PSDs (σ_{psd}) have been done using the same beams already mentioned. The distance between the target and the PSDs was 190 mm, no gas was used in the ionization chamber and the entrance window was removed for this test. Two 1 mm diameter needles were fixed at different positions perpendicular to the active strip of each PSD. When these detectors were uniformly impinged by the incident particles the needles produced in all cases clear dips in the position spectra that allowed us to obtain reliable calibration data. By application of this procedure the intrinsic position resolutions were estimated to be 1 mm, which in this case corresponds to an uncertainty of 0.3° in the emission

angle. The obtained values of the position resolution are in agreement with those reported by the manufacturers [3,4].

In order to determine the angular uncertainty produced by the ionization chamber gas, $\sigma_{gas}(P)$, several measurements have been done at different pressures of P10 gas using the mentioned beams. Three slits covering the angular ranges $\Delta\theta = 1.0^\circ$, 0.5° and 1.5° over PSDs A, B and C, respectively, were fixed to the entrance window of the detection system. The ionization chamber was operated in a range of pressures from high vacuum (10^{-6} mbar) up to 270 mbar depending on the detected particles. Since all the other factors do not vary with the pressure, the contribution due to the ionization gas at a given pressure P was obtained from measurements taken at some values and at $P \approx 0$ mbar (high vacuum), using

$$\sigma^2_{gas}(P) = \sigma^2(P) - \sigma^2(0) \quad (1)$$

It should be pointed out that for the present measurements the FWHM σ used in Eq. (1) includes not only the contributions mentioned above, but also two other pressure-independent contributions, namely, those arising from the geometrical projection of the slits on the PSDs' strips and from slit scattering. It has been verified that the measured total FWHM when the ionization chamber was in vacuum, $\sigma(0)$, is consistent with the results of calculations that take into account the experimental resolution of the PSDs, and the straggling caused by the entrance Mylar window (which was estimated using the code SRIM [5]). Fig. 2 summarizes the behavior of the experimentally obtained values of $\sigma_{gas}(P)$ as a function of P for different ions. They are very well reproduced by simulations carried out with SRIM, which are shown in the same figure.

In summary, taking into account all contributions, the total angular FWHM under the most adverse condition (i.e., when ions lose most of their energy in the gas) was found to be less than 0.8°. This means that particles emitted at an angle θ will be actually detected within a range of $\theta \pm 0.3^\circ$ (with 68% of probability).

3.2. Elastic scattering and alpha particle production measurements in the ^{7}Li+^{27}Al system

The performance of the detection system has also been examined comparing the results of elastic scattering with previous data and measuring alpha particle production cross-sections, both in the ^{7}Li+^{27}Al system.

Fig. 3 shows a bi-dimensional E_{res}–ΔE spectrum taken at $E_{lab} = 18$ MeV, where the E_{res} information is given by the central PSD covering an angular range from 40° to 50°. In this spectrum there is a clear separation of the elastic peak ($Z=3$), avoiding the interference with other detected particles.

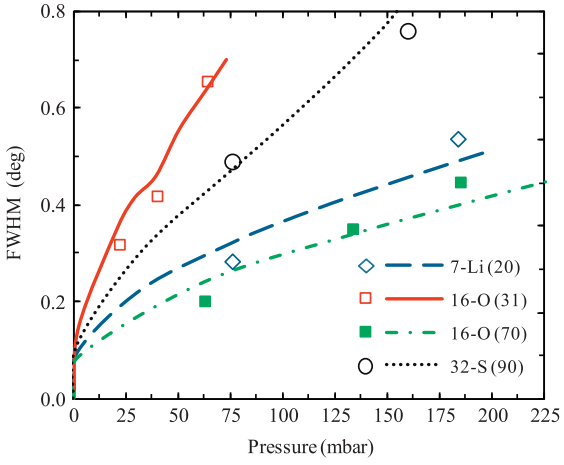

Fig. 2. Measured (symbols) and estimated (lines) angular straggling due to gas effects for PSD B. The bombarding energies for each beam, in MeV, are quoted in parenthesis.

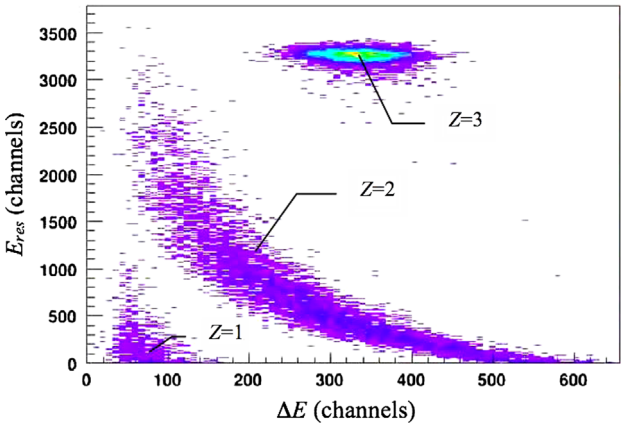

Fig. 3. E_{res}–ΔE spectrum, for the ^{7}Li+^{27}Al system at $E_{lab} = 18$ MeV obtained with PSD B centered at 45°.

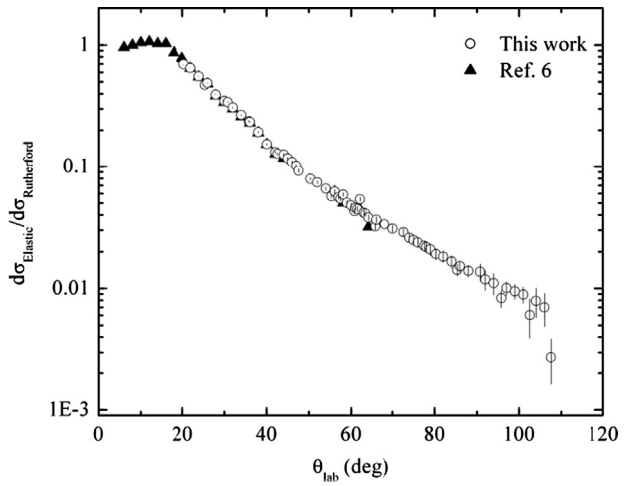

Fig. 4. Angular distribution for ^{7}Li+^{27}Al elastic scattering at laboratory energy of 18 MeV from this work and Ref. 6. A variable number of bins for each PSD was used.

In the off-line analysis, each PSD active strip was divided into a variable number of bins in order to optimize the determination of the angular distribution. Since each PSD covers an angular range of approximately 10°, and we have shown that the angular straggling is in any case less than $\Delta\theta = 1^\circ$, therefore the number of bins can be selected up to a maximum of ten. The angular calibration (i.e., the determination of the correspondence between each bin and a given angular position) has been obtained using the relative position of the aforementioned needles respect to the beam direction.

In order to obtain a reliable normalization, the angular distribution of the elastic scattering cross-section of the ^{16}O+^{197}Au system at a sub Coulomb barrier energy ($E_{lab} = 42$ MeV) was measured. Since this cross-section must follow the Rutherford formula, the solid angle ratio between each PSD bin and a monitor detector was obtained; independently of the target thickness (which usually has a high uncertainty) and the beam current. This ratio is then used for normalization purposes.

In Fig. 4, we show the cross-section angular distribution for ^{7}Li +^{27}Al elastic scattering at the laboratory energy of 18 MeV. In this same figure, prior experimental data [6] are also included for comparison. A very good agreement is observed between both data series. The large angular acceptance of this device allows covering regions of interest (backward angles in the above

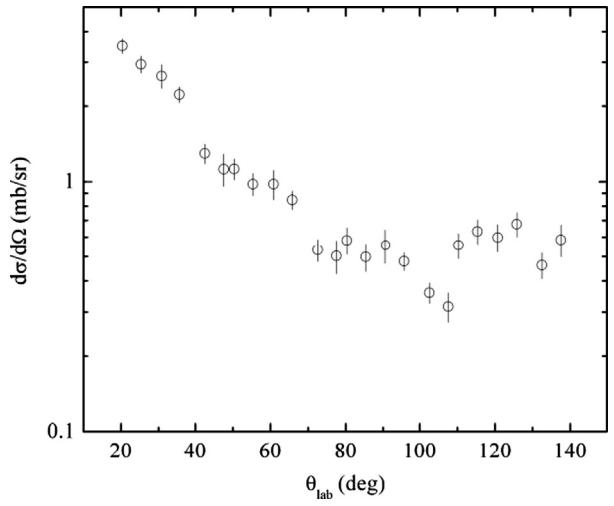

Fig. 5. Angular distribution of the alpha particle production cross-section for the ^{7}Li+^{27}Al system at laboratory energy of 18 MeV.

mentioned case) where measurements with other detection systems proved to be very time-consuming.

Relying on the previously performed tests, the data obtained for the observed alpha particles produced in the ^{7}Li+^{27}Al system were further analyzed. The signals derived from these events at $E_{lab}=18$ MeV appeared clearly separated, as seen in Fig. 3. These particles may come from different reaction mechanisms. Measurements of their angular distributions can be useful to evaluate the relative importance of each process, the most important being: non-capture breakup (^{4}He+^{3}H+^{27}Al), capture or sequential breakup (^{4}He+^{2}H+^{28}Al), *t*-transfer and/or incomplete fusion (^{4}He +^{30}Si) and fusion-evaporation (^{34}S*→^{4}He+*x*n+$^{30-x}$Si).

As an example, in Fig. 5 we present the corresponding angular distribution for the ^{7}Li+^{27}Al system at the laboratory energy of 18 MeV. A deeper analysis of the mentioned alpha particle production processes, in particular breakup, is out of the scope of this publication and is the subject of current research in our group [7,8].

4. Conclusions

In this paper we present the first tests of a new detection system suitable for time-optimized angular distribution measurements and particle identification. This broad angular acceptance device has a reasonable energy resolution of around 3% at normal operation conditions and an adequate angular resolution (better than 1°), which allowed us to reproduce previously measured elastic scattering cross-sections in our test experiments.

We also obtained an angular distribution of alpha particles produced in the ^{7}Li+^{27}Al system. This result encouraged us to launch, at the TANDAR facility, a research program on alpha particle production in reactions induced by weakly bound nuclei.

Acknowledgments

This work was supported by CONICET and UNSAM grants.

References

[1] G.F. Knoll, Radiation Detection and Measurement, Third ed., J. Wiley, New York, 2000.
[2] R.G. Liberman, et al., Nuclear Instruments and Methods in Physics Research 565 (2006) 686.
[3] ORTEC P-Series Detectors Specifications, ⟨http://www.ortec-online.com⟩.
[4] Canberra Position PIP Detectors Specifications, ⟨http://www.canberra.com⟩.
[5] J.F. Ziegler, SRIM: The Stopping and Range of Ions in Matter, ⟨http://www.srim.org⟩.
[6] J.M. Figueira, et al., Physical Review C 73 (2006) 054603.
[7] D. Martinez Heimann, et al., AIP Conference Proceedings 1098 (2009) 275.
[8] P.F.F. Carnelli et al., in preparation.